Quasiparticlelike Peaks, Kinks, and Electron-Phonon Coupling at the $(\pi, 0)$ Regions in the CMR Oxide $La_{2-2x}Sr_{1+2x}Mn_2O_7$

Z. Sun,[1,2] Y.-D. Chuang,[2] A. V. Fedorov,[2] J. F. Douglas,[1] D. Reznik,[3] F. Weber,[3] N. Aliouane,[4] D. N. Argyriou,[4] H. Zheng,[5] J. F. Mitchell,[5] T. Kimura,[6,*] Y. Tokura,[6] A. Revcolevschi,[7] and D. S. Dessau[1]

[1]*Department of Physics, University of Colorado, Boulder, Colorado 80309, USA*
[2]*Advanced Light Source, Lawrence Berkeley National Laboratory, Berkeley, California 94720, USA*
[3]*Forschungszentrum Karlsruhe, Institut für Festkörphysik, Postfach 3640, D-76021 Karlsruhe, Germany*
[4]*Hahn-Meitner-Institut, Glienicket Strasse 100, Berlin D-14109, Germany*
[5]*Materials Science Division, Argonne National Laboratory, Argonne, Illinois 60439, USA*
[6]*Department of Applied Physics, University of Tokyo, Tokyo 113-8656, Japan*
[7]*Laboratoire de Physico-Chimie de l'Etat Solide, University of Paris Sud-11, 91405 Orsay Cedex, France*

(Received 19 October 2005; published 31 July 2006)

Using angle-resolved photoemission, we have observed sharp quasiparticlelike peaks in the prototypical layered manganite $La_{2-2x}Sr_{1+2x}Mn_2O_7$ ($x = 0.36, 0.38$). We focus on the $(\pi, 0)$ regions of k space and study their electronic scattering rates and dispersion kinks, uncovering bilayer-split bands, the critical energy scales, momentum scales, and strengths of the interactions that renormalize the electrons. To identify these bosons, we measured phonon dispersions in the energy range of the kink by inelastic neutron scattering, finding a good match in both energy and momentum to the oxygen bond-stretching phonons.

DOI: 10.1103/PhysRevLett.97.056401 PACS numbers: 71.18.+y, 71.38.−k, 78.70.Nx, 79.60.−i

The exotic physics in condensed matter systems, such as high-T_c superconductivity in cuprates [1] and colossal magnetoresistance (CMR) in manganites [2,3], is due to strong many-body interactions of unknown origin. Relevant interactions are either electron-electron or electron-boson, where the boson is a collective excitation such as a magnon or, as in the case of conventional superconductivity [4], a phonon. These interactions are typically described as ''dressing'' the electrons to create quasiparticles, the properties of which determine physical quantities such as electrical and thermal conductivity. In certain cases such as one-dimensional ''Luttinger liquids'' [5] and possibly cuprates [6] and manganites [7], the electronic correlations are so strong that the quasiparticle concept falls apart, and only broad and strongly damped electronic excitations have been observed. A side effect of this is that the absence of the quasiparticles gives experimentalists fewer windows into the interactions responsible for the behavior of the system.

Many-body interactions in manganites are expected to be strong and include the coupling to other electrons plus collective modes such as phonons [8,9], magnons [10,11], and orbitons [12,13]; the details of how these modes couple to the electrons, however, have been almost completely unexplored. In essence, we do not know which modes are most relevant or how strongly they couple to the electrons.

$La_{2-2x}Sr_{1+2x}Mn_2O_7$ is a naturally layered compound with two MnO_2 planes per unit cell, with the physical properties dominated by these bilayers [14]. The $x = 0.36$–0.4 samples have a transition from a high-temperature paramagnetic insulating state to a low-temperature ferromagnetic metallic state at $T_c \sim 120$–130 K. To uncover the properties of electrons and their interactions with bosonic modes in these compounds, we take advantage of two powerful energy and momentum-resolved techniques, angle-resolved photoemission spectroscopy (ARPES) and inelastic neutron scattering (INS) to individually probe the electrons and bosons throughout the zone, respectively. This powerful combination gives unprecedented clarity into the many-body interactions in the CMR compounds. We observed sharp quasiparticlelike peaks using ARPES, which opens a window for us to study electronic dispersions and scattering rates as well as how the electrons are renormalized by bosonic modes. Phonon dispersions were measured by INS, which have a good match in both energy and momentum to that which should couple to electrons, indicating the relevance of phonons to the interactions in manganites.

The ARPES experiments were performed at beam line 12.0.1 of the Advanced Light Source (ALS), Berkeley, using a Scienta SES100 electron analyzer under a vacuum better than 3×10^{-11} torr. All samples were cleaved *in situ* at 20 K. The combined instrumental energy resolution of experiments was better than 20 meV and the momentum resolution was about 2% of the zone edge ($0.02\pi/a$). The neutron scattering experiments were performed on the 1 T triple axis spectrometer at the ORPHEE reactor at Saclay utilizing the 220 reflection of copper as the monochromator and the 002 reflection of pyrolytic graphite. The sample was mounted in a closed-cycle refrigerator with the measurements performed at 11 K.

The electronic spectral function is determined from ARPES data. Figure 1(a) illustrates the typical Fermi surface of $La_{2-2x}Sr_{1+2x}Mn_2O_7$ [7]. Theoretically, there is a small piece at the zone center consisting of primarily out-of-plane $d_{3z^2-r^2}$ Mn-O states, while the large hole pockets

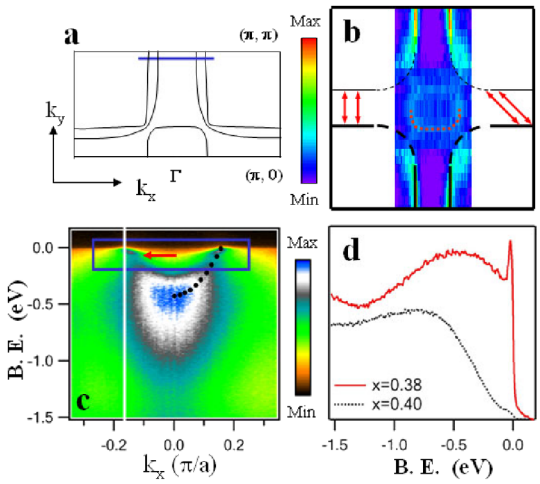

FIG. 1 (color online). Low-temperature ($T = 20$ K) ARPES data from $La_{2-2x}Sr_{1+2x}Mn_2O_7$ ($x = 0.38$). (a) A representative Fermi surface, after Ref. [7]. (b) The spectral weight at E_F over much of the first Brillouin zone and Fermi surfaces of the antibonding band (black lines) and $d_{3z^2-r^2}$ Mn-O states (dots near the zone center). The arrows show 100 (left) and 110 (right) nesting vectors. (c) Binding energy versus momentum (π/a) image plot of the antibonding band from the 0.9π slice [as indicated in (a)]; black dots indicate the bare band dispersion and were determined from a combination of fits to EDCs (deeper energies) and MDCs (near E_F). (d) EDC at k_F indicated by the vertical white line in (c) and a typical low-temperature EDC at k_F (black dotted line) in $x = 0.4$ compounds.

centered at the zone corners are due to bilayer-split in-plane $d_{x^2-y^2}$ Mn-O states [7]. These in-plane states, which are expected to be more important for the transport and magnetic properties of these layered materials, are the focus of this Letter. All previous work had been unable to resolve the bilayer splitting. In this work, we discovered we could selectively pick up either the bonding or antibonding bands near $(\pi, 0)$ regions by tuning the matrix elements, which allows a highly accurate analysis of data. We empirically found that bonding and antibonding portions of the bilayer-split bands are emphasized with 73 and 56 eV photons, respectively. Similar strong photon energy dependence of electronic bands has been observed in a layered cuprate [15,16], and it has become common in ARPES studies. The spectral weight at the Fermi energy taken using 56 eV photons at $T = 20$ K is shown in Fig. 1(b), giving a (matrix-element modulated) experimental mapping of the 2D Fermi surface. The weak feature around the zone center as indicated by the dots in Fig. 1(b) is consistent with the prediction of the small electron pocket. Here we focus on data along the line $(k_x, 09\pi/a)$ in Fig. 1(a). Figure 1(c) shows a wide binding energy scan of the antibonding band as a function of k_x at $T = 20$ K, exhibiting a clear parabolic dispersive feature with maximal spectral weight around the binding energy 0.4 eV. The bonding band (not shown) has a similar dispersive feature and reaches 400 meV deeper binding energy. The black dots superimposed on the right half of the data show this wide-scale dispersion clearly. Near E_F (below the arrow), the dispersive feature is sharp and heavily renormalized from the parabolic dispersion, indicating important many-body effects.

An energy distribution curve (EDC) taken at $k = k_F$ from these data [vertical white line in Fig. 1(c)] is plotted in Fig. 1(d). Near E_F, there is a clear and well-resolved quasiparticlelike peak—the first such observation in antinodal states in a CMR oxide. This observation by itself has important ramifications for the study of electronic correlations in low-dimensional systems such as the layered manganites, as certain important classes of models of correlated electrons [5,6] require the absence of such quasiparticles. Compared to data on $La_{2-2x}Sr_{1+2x}Mn_2O_7$ ($x = 0.4$) which have very small spectral weight near E_F [7,17–19] [black curve in Fig. 1(d)], the quasiparticle peak here is not likely due to improved sample quality issues but rather due to the absence of antiferromagnetic (AF) canting [20] in the $x = 0.36$ and 0.38 samples, which tends to make these samples electronically more three-dimensional than samples with $x = 0.40$ and above, which have AF canting between the planes. Within the double-exchange picture, this AF canting should reduce the coupling between the planes, making the 0.4 and above samples more two-dimensional [21]. This trend is consistent with that observed in the cobaltates [22] and ruthenates [23], in which it has been argued that a high dimensionality favors more quasiparticle spectral weight. We have measured many high-quality bilayer manganite samples in the doping range from $x = 0.36$ to $x = 0.5$ under the same experimental conditions. The evolution of the near E_F spectral weight is consistent with the picture of dimensional crossover with doping change. We suggest that optical conductivity studies [24] of the low energy Drude peak as a function of doping and polarization may also be able to address this issue.

The results in Fig. 1 indicate that the $x = 0.36$–0.38 samples are more "normal" than the 0.40 samples; i.e., at low temperature they have significant quasiparticle weight and no clear pseudogap—behavior expected for a metal. Therefore, we believe that these samples and not the $x = 0.40$ samples should be the starting material to discuss layered manganite physics. The electronic structure of this prototypical manganite is for the first time laid out in this Letter.

The clear presence of quasiparticlelike peaks gives us a new and detailed window into the electronic correlations in the manganites. Figure 2 shows details of the near-Fermi energy region of the data. Figure 2(a) shows the antibonding data as a function of k_x. The solid squares in Fig. 2(b) show the dispersion relation, which were determined from fits of momentum distribution curves (MDCs) with a Lorentzian line shape on top of a small monotonically varying background, while the solid circles show the results from a similar analysis of bonding band data [25] (upper axis—note the different scale from the bottom axis). An s-shaped kink structure, deviating from the non-

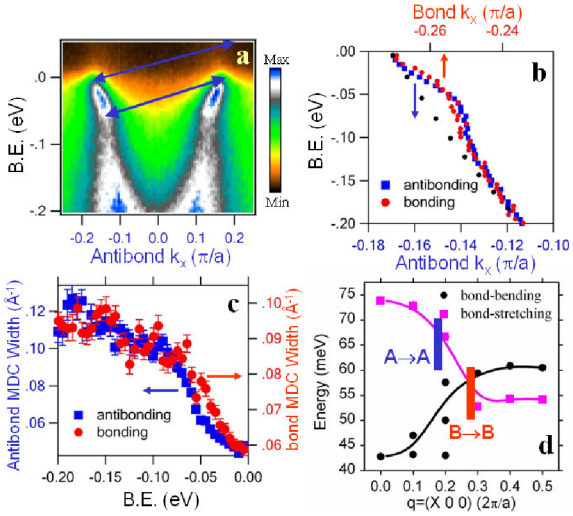

FIG. 2 (color online). Electron and phonon dispersion relations and scattering rates. (a) Energy versus momentum image plot of the antibonding electron band from the 0.9π slice [the frame in Fig. 1(c)]. (b) MDC derived E vs k dispersion of antibonding states and bonding states compared to a parabolic fit to the deeper lying antibonding dispersion (black dots). (c) MDC full widths versus energy for antibonding and bonding states. (d) Phonon dispersion relations from neutron scattering from the bond-stretching and bond-bending modes of even symmetry. The bond-bending vibration contributes to multiple modes at some wave vectors because it mixes with other vibrations. The lines are guides to the eye. Electron kink scales and nesting q vectors for the antibonding (A → A) and bonding band (B → B) are also included.

interacting parabolic dispersion (black dots), can be clearly seen for both bands. These deviations are due to the many-body effects and, in the language of many-body physics, are due to the real part of the electron self-energy $\mathrm{Re}\sum$. The slopes of the renormalized and noninteracting dispersions near E_F give the renormalized and bare Fermi velocities, respectively. In a simple electron-boson coupling model, their ratio can be parametrized as $1 + \lambda$, where λ is a measure of the electron-boson coupling strength (also termed the mass enhancement). Since the ratio of the low energy slopes is approximately 2, this would imply $\lambda \sim 1$ for both bonding and antibonding bands. We also note that specific-heat data have indicated similar values of the coupling strengths [26,27], though this analysis is much less direct as it is based on a comparison to theoretical band structure data.

Typically, the low-temperature metallic state of the manganites is considered to be a rather standard metal without strong correlation effects. The coupling strength λ discovered here tells a different story, however. This is in the intermediate-to-strong coupling regime [28] and is on the precipice such that a minor perturbation in parameters giving a small increase in the coupling strength may lead to polaronic localization. Therefore, these couplings may likely be responsible for the metal-insulator transition which is at the heart of the CMR problem.

The identity of the important boson mode(s) can be determined from these dispersions. Based on the maximum in $\mathrm{Re}\sum$ at about 50–60 meV, we estimate that the critical energy of the boson mode(s) is around 60–70 meV for the antibonding band and about 50–60 meV for the bonding band [29]. A clear step increase in the scattering rates centered at the same energy scales are observed [Fig. 2(c)]. This self-consistency gives great confidence in the assignment of the critical energy scales to the data. Modes at other energy scales will, of course, have some relevance as well, but as evidenced by the kink data they will couple to the electrons less strongly than modes near 60 meV.

Various proposals for the important mode coupling in the manganites have been made, including phonons [8,9], magnons [10,11], and orbitons [12,18]. A key point is that the strongly nested Fermi surface should be highly susceptible to a mode with a momentum transfer equal to the nesting vector $q \sim 0.17 \times (2\pi/a, 0)$ or $0.17 \times (2\pi/a, 2\pi/a)$ for the antibonding band and $q \sim 0.27 \times (2\pi/a, 0)$ or $0.27 \times (2\pi/a, 2\pi/a)$ for the bonding band. The arrows in Fig. 2(a) indicate the corresponding electron scattering within the antibonding band with $q \sim 0.17 \times (2\pi/a, 0)$. At these q vectors, the excitation energy of magnons is ~30 meV [11], and orbitons are larger than 100 meV over the entire zone [18] and so are in disagreement with the critical energy scales we observed here. However, there are longitudinal optical phonons that couple to charge fluctuations in the Mn-O layers exactly in this momentum and energy range, which makes these phonons a good candidate for the dominant coupling.

We performed neutron scattering measurements on $La_{2-2x}Sr_{1+2x}Mn_2O_7$ ($x = 0.4$) to determine the phonon structures and dispersion relations of the longitudinal bond-stretching and bond-bending phonons, as shown in Fig. 2(d). At this time, only data along X00 are available, although XX0 (Jahn-Teller) phonons also will likely be relevant. The phonon mode of primary interest is the bond-stretching mode, the dispersion of which is quite universal for perovskite oxides and approximately independent of doping level [30]. Raman spectra have also proven that phonons in $La_{2-2x}Sr_{1+2x}Mn_2O_7$ ($0.38 \leq x \leq 1$) are not very sensitive to doping [31]. Therefore, neutron measurements on $x = 0.4$ samples should be a fairly good approximation for $x = 0.38$ samples. Both even and odd modes with respect to the bilayer structure of $La_{2-2x}Sr_{1+2x}Mn_2O_7$ have been measured. Only even phonons are shown here—the odd phonons have similar dispersions but are a few meV lower. Overlaid with the phonon dispersion curves on this plot are the kink energy scales from the ARPES data, plotted at the respective q vectors where energy-momentum conservation allows the phonons to scatter from intraband transition (A → A and B → B). Interband transitions such as A → B will show up at an intermediate position and are not included on the graph. It is seen that both the kink energies and nesting vectors of the electrons match closely with the phonon energies and q values, giving confidence that it is these phonons which have dominant

coupling to the electrons along this direction. Especially important are the bond-stretching phonons, which should couple most strongly to the bonding and antibonding electrons (the bond-bending phonons may couple to the bonding electrons as well). The downward dispersion of the bond-stretching phonons also is seen to match well with the electron kink data and is in contrast with that found for the upward-dispersive magnons [11]. In fact, the downward dispersion of the bond-stretching phonons has long been considered an anomaly in manganites and other perovskites, as a simple shell-model predicts that the bond-stretch phonons should have an upward dispersion [32]. The downward dispersion is seen to occur at the same q values where the electron nesting occurs, so future studies might consider whether the coupling to the electrons renormalizes these phonon properties as well.

The coupling of electrons to the bond-stretching phonon branch has also been considered to be important in the cuprates [33]. The studies of electron-phonon coupling in manganites may provide opportunities to uncover the roles phonons play not only in the CMR effect but also in the pairing of electrons in high-T_c cuprates.

We are grateful to T. Devereaux, T. Egami, N. Furukawa, and J. Zhang for helpful discussions. This work was supported by DOE Grant No. DE-FG02-03ER46066 and by NSF Grant No. DMR0402814. The ALS is operated by the DOE Office of Basic Energy Sciences.

Note added.—After completion of this work, we became aware of an ARPES study on $x = 0.4$ bilayer manganites by Mannella *et al.* [19]. They uncovered quasiparticlelike peaks in the ''nodal'' or zone-diagonal direction but no quasiparticles at the antinode. Their thesis is of a ''nodal Fermi liquid'' of such a generic origin that it transcends both cuprates and manganites. The observation of strong quasiparticlelike peaks in the antinodal regime in this work indicates that the 0.36 and 0.38 samples cannot be classified as a nodal Fermi liquid. We argued that these doping-dependent differences may be related to AF canting between the ferromagnetic bilayer planes which should effectively change their dimensionality and hence their propensity to support quasiparticles. We also note that they used the EDC dispersion to estimate quasiparticle mass enhancements, compared to the more standard MDC-based method we used. If we use an EDC method, we get a mass enhancement of ~5 from our data, though we feel that this overestimates the coupling strengths and is inconsistent with the specific heat data.

*Present address: Bell Laboratories, Lucent Technologies, Murray Hill, NJ 07974, USA.

[1] J. G. Bednorz and K. A. Müller, Z. Phys. B **64**, 189 (1986).
[2] *Colossal Magnetoresistive Oxides*, Advances in Condensed Matter Physics Science Vol. 2, edited by Y. Tokura (Gordon and Breach, Amsterdam, 2000).
[3] *Colossal Magnetoresistive Manganites*, edited by T. Chatterji (Kluwer Academic, Dordrecht, The Netherlands, 2004).
[4] *Theory of Superconductivity*, edited by J. R. Schrieffer (Perseus Books, Boulder, CO, 1999).
[5] J. Voit, Rep. Prog. Phys. **58**, 977 (1995).
[6] P. W. Anderson, *The Theory of Superconductivity in the High-Tc Cuprates* (Princeton University, Princeton, NJ, 1997).
[7] D. S. Dessau *et al.*, Phys. Rev. Lett. **81**, 192 (1998).
[8] V. Perebeinos and P. B. Allen, Phys. Rev. Lett. **85**, 5178 (2000).
[9] A. J. Millis *et al.*, Phys. Rev. Lett. **74**, 5144 (1995).
[10] M. Jaime *et al.*, Phys. Rev. B **58**, R5901 (1998).
[11] K. Hirota *et al.*, Phys. Rev. B **65**, 064414 (2002).
[12] J. van den Brink *et al.*, Phys. Rev. Lett. **85**, 5174 (2000).
[13] E. Saitoh *et al.*, Nature (London) **410**, 180 (2001).
[14] J. F. Mitchell *et al.*, J. Phys. Chem. B **105**, 10 731 (2001).
[15] Y. D. Chuang *et al.*, Phys. Rev. B **69**, 094515 (2004).
[16] M. Lindroos *et al.*, Phys. Rev. B **65**, 054514 (2002).
[17] Y. D. Chuang *et al.*, Science **292**, 1509 (2001).
[18] T. Saitoh *et al.*, Phys. Rev. B **62**, 1039 (2000).
[19] N. Mannella *et al.*, Nature (London) **438**, 474 (2005).
[20] M. Kubota *et al.*, J. Phys. Soc. Jpn. **69**, 1606 (2000).
[21] According to the double-exchange mechanism, the antiferromagnetism in the c-axis direction in high doping levels is expected to strongly reduce the electron's hopping in this direction.
[22] T. Valla *et al.*, Nature (London) **417**, 627 (2002).
[23] S.-C. Wang *et al.*, Phys. Rev. Lett. **92**, 137002 (2004).
[24] T. Ishikawa *et al.*, Phys. Rev. B **62**, 12 354 (2000).
[25] Bonding band data were from an 0.36 doped sample from which we obtained better statistics, though the same energy scale as from 0.38 data.
[26] T. Okuda *et al.*, Phys. Rev. Lett. **81**, 3203 (1998).
[27] B. F. Woodfield *et al.*, Phys. Rev. Lett. **78**, 3201 (1997).
[28] G. D. Mahan, *Many Particle Physics* (Plenum, New York, 1990), Chap. 6.
[29] In the limit of zero broadening, we expect the kink energy to asymptotically approach the boson energy scale from below. In the real case with finite signal strength and peak broadening, the kink will never fully approach the boson energy scale, and so the kink energy will slightly underestimate the mode energy. We therefore consider the kink energy ~60 meV to be the lower limit of the boson energy scale for the antibonding band and ~50 meV to be the lower limit for the antibonding band. The upper limit of the boson scale should be about 10 meV greater, where we can clearly distinguish a lone higher energy feature.
[30] M. Braden *et al.*, Physica (Amsterdam) **378C–381C**, 89 (2002).
[31] I. Guedes *et al.*, J. Raman Spectrosc. **31**, 1013 (2000).
[32] W. Reichardt and M. Braden, Physica (Amsterdam) **263B–264B**, 416 (1999).
[33] A. Lanzara *et al.*, Nature (London) **412**, 510 (2001).